Epithelial organization and cyst lumen expansion require efficient Sec13–Sec31-driven secretion

Anna K. Townley[1,*], Katy Schmidt[1,*,‡], Lorna Hodgson[1] and David J. Stephens[1,§]

[1]Cell Biology Laboratories, School of Biochemistry, Medical Sciences Building, University of Bristol, University Walk, Bristol, BS8 1TD, UK

*These authors contributed equally to this work
‡Present address: Max F. Perutz Laboratories Dr. Bohr Gasse 9/3 1030 Wien, Austria
§Author for correspondence (david.stephens@bristol.ac.uk)

Accepted 26 October 2011
Journal of Cell Science 125, 673–684

doi: 10.1242/jcs.091355

Summary

Epithelial morphogenesis is directed by interactions with the underlying extracellular matrix. Secretion of collagen and other matrix components requires efficient coat complex II (COPII) vesicle formation at the endoplasmic reticulum. Here, we show that suppression of the outer layer COPII component, Sec13, in zebrafish embryos results in a disorganized gut epithelium. In human intestinal epithelial cells (Caco-2), Sec13 depletion causes defective epithelial polarity and organization on permeable supports. Defects are seen in the ability of cells to adhere to the substrate, form a monolayer and form intercellular junctions. When embedded in a three-dimensional matrix, Sec13-depleted Caco-2 cells form cysts but, unlike controls, are defective in lumen expansion. Incorporation of primary fibroblasts within the three-dimensional culture substantially restores normal morphogenesis. We conclude that efficient COPII-dependent secretion, notably assembly of Sec13–Sec31, is required to drive epithelial morphogenesis in both two- and three-dimensional cultures in vitro, as well as in vivo. Our results provide insight into the role of COPII in epithelial morphogenesis and have implications for the interpretation of epithelial polarity and organization assays in cell culture.

Key words: COPII, ER export, Epithelial organization

Introduction

Epithelial morphogenesis requires formation of cell–substrate contacts to enable polarization of cells. Cell–substrate contacts are defined as interactions between cells and a specialized extracellular matrix (ECM), the basal lamina, which consists mainly of collagen and laminin. The ECM is generally secreted by epithelial cells. Elucidating the molecular mechanisms underlying the interactions between epithelial cells and basal lamina, culminating in formation of an epithelial sheet or a tube of cells, is crucial for our understanding of development, organ function, and the onset and progression of disease (reviewed by Bryant and Mostov, 2008). Membrane traffic is essential to establish and maintain cell polarity through apical and basal targeting of proteins as well as through directed recycling of components between these membrane domains (Mellman and Nelson, 2008). Increasing evidence shows that directed secretion of ECM is a key requirement in establishment of polarity. Membrane trafficking through the early secretory pathway has been implicated in tube or lumen formation in several systems in vivo (Tsarouhas et al., 2007; Grieder et al., 2008; Jayaram et al., 2008; Norum et al., 2010). For example, the *Drosophila* mutants *haunted* and *ghost* show defects in epithelial polarity as well as in secretion into the luminal matrix of the trachea and cuticle deposition. The *haunted* and *ghost* genes encode the coat complex II (COPII) proteins Sec23 and Sec24, respectively (Norum et al., 2010). The COPII component Sar1 has been shown to be required for luminal matrix assembly and tube expansion of *Drosophila* trachea (Tsarouhas et al., 2007). More recently, Sec24 has been shown to be essential for lumen expansion in tracheal development in a cell autonomous manner (Forster et al., 2010). Extensive secretion of atypically large cargo is also essential for cuticle formation, which relies on *sar1*, *sec23* and *sec13* function (Abrams and Andrew, 2005). In addition, it has been shown that expression of COPII components is upregulated during development of the *Drosophila* salivary gland (Abrams and Andrew, 2005), a highly tubulated organ that has a high secretory load.

The COPII coat (Barlowe et al., 1994) directs cargo selection and budding of transport carriers from the ER membrane (reviewed by Hughes and Stephens, 2008). COPII assembly is triggered by Sec12-dependent activation of the small GTPase Sar1 (d'Enfert et al., 1991), which recruits the heterodimeric major cargo selection module Sec23–Sec24 (Kuehn et al., 1998) to form the pre-budding complex. These pre-budding complexes subsequently recruit an additional layer of the COPII vesicle coat, Sec13–Sec31, which enhances GTP hydrolysis on Sar1 and completes budding of the vesicles (Salama et al., 1997; Antonny et al., 2001; Townley et al., 2008). COPII vesicles formed in vitro are typically 60–80 nm in size (Matsuoka et al., 1998; Antonny et al., 2003). The cages that spontaneously assemble from purified Sec13–Sec31 (Stagg et al., 2006) and those that are seen in or purified from cells (Aridor et al., 1999; Matsuoka et al., 2001) are also 60 nm in size. This presents an inherent problem for the packaging of large secretory cargo and, consequently, for characteristic components of the basal lamina, notably linear rod-like molecules such as fibrillar procollagen type I (~300 nm) (Canty and Kadler, 2005), and potentially for other ECM molecules, e.g. laminin (up to 120 nm) (Beck et al., 1990) and perlecan (up to 200 nm) (Farach-Carson and Carson, 2007).

We recently established that RNA interference (RNAi)-mediated suppression of Sec13 results in depletion of the entire outer layer of the COPII vesicle coat complex and causes a selective defect in collagen secretion (Townley et al., 2008) in development of the craniofacial skeleton but probably also of other large ECM molecules (Townley and Stephens, 2009). Because of their shape and size, large cargos including these ECM components are more likely to rely on a strengthened and persistent vesicle coat than small soluble molecules would be. This implies a role for the outer COPII coat, Sec13–Sec31, in scaffolding and stabilizing transport carriers containing atypically large cargo (Fromme and Schekman, 2005; Townley and Stephens, 2009). A current model proposes that export of large cargo requires highly efficient coupling between the inner COPII layer, Sar1 with Sec23–Sec24, and the COPII outer layer, Sec13–Sec31 (Schmidt and Stephens, 2010). Mutation of Sec23A results in inefficient assembly of the full COPII coat, with the resulting defects in collagen secretion from chondrocytes causing cranio-lenticulo-sutural dysplasia (Boyadjiev et al., 2006; Bi et al., 2007; Fromme et al., 2007).

In order to determine whether Sec13–Sec31 is generally required for the transport of large cargo as opposed to a restricted action in chondrogenesis, we examined the effects of knockdown of Sec13–Sec31 in gut morphogenesis in zebrafish embryos and an intestinal epithelial cell culture system. Establishment of a basal lamina coincides with generation and polarization of an epithelial cell layer, which provides an ideal read-out for effective secretion of large cargo both, in vitro and in vivo. The most notable defect observed in the intestine of Sec13–Sec31-depleted zebrafish embryos was the disorganization of the intestinal epithelium along with a restricted gut lumen. We therefore sought to define the functional necessity of Sec13–Sec31 in epithelial polarity and organization of Caco-2 (human colon cancer) cells in vitro. Here, we show that on-going efficient COPII-dependent secretion is essential during epithelial morphogenesis in vitro and in vivo. These data demonstrate the importance of careful interpretation of experimental outcomes from two- and three-dimensional (2D and 3D, respectively) epithelial cell culture systems in which defined phenotypes could arise from defects in secretion rather than the primary experimental manipulation.

Results

Defective lumen expansion in zebrafish Sec13 morphants

We analyzed the organization of intestinal epithelia in Sec13 morphant zebrafish embryos in order to define the role of Sec13–Sec31-dependent transport for establishment of the basal lamina in intestinal morphogenesis. Two translation-blocking morpholino oligonucleotides targeted against Sec13 were used (Sec13-1 and Sec13-2); the phenotypes were indistinguishable using either of them (see also Townley et al., 2008). Results from only one morpholino (Sec13-2) are shown in Fig. 1. The intestinal phenotype of all zebrafish included in this study was defined by showing pectoral fin defects, as described previously (Townley et al., 2008). The intestinal epithelium of Sec13 morphants was disorganized compared with age-matched controls on sections taken from the same level along the cranio–caudal length of the embryos. Sec13-suppressed zebrafish showed inefficient monolayer formation and dramatically restricted intestinal lumen expansion (Fig. 1A), suggesting that the polarization of epithelial cells might be affected by the reduction in Sec13 levels. To evaluate the cellular phenotype of the Sec13 morphant gut lining, we conducted electron microscopy on thin sections from the same samples.

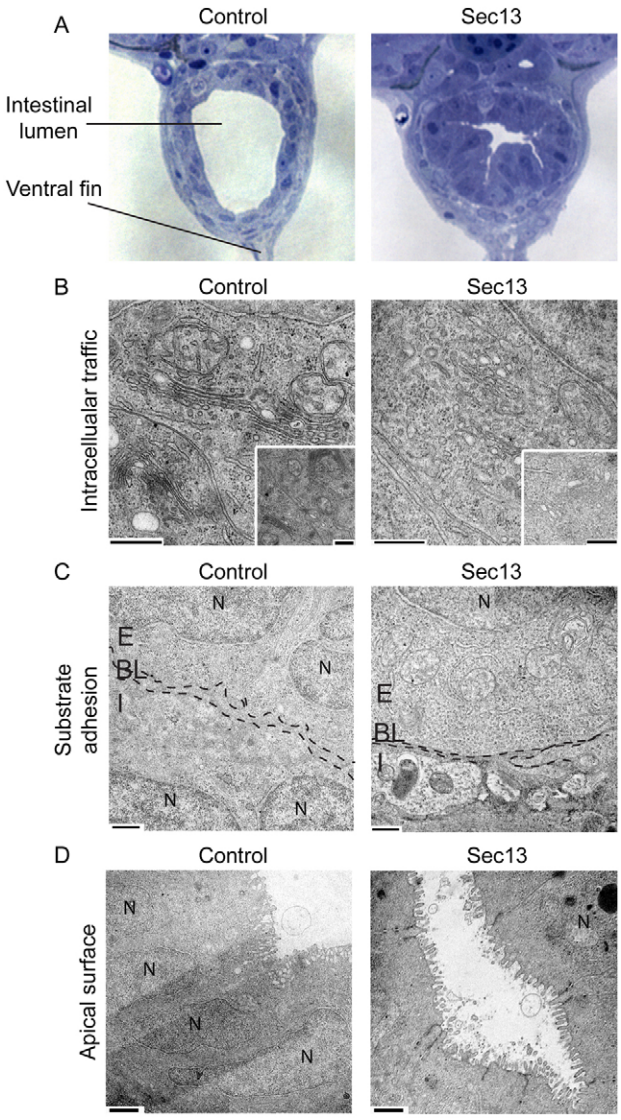

Fig. 1. Disorganization and limited expansion of the zebrafish gut lumen following Sec13 suppression. (**A**) Transverse sections through the gut of 5 dpf zebrafish embryos injected with control (left) or Sec13 morpholinos (right). Sections (1 μm) were taken from a comparable level along the cranio–caudal axis of age-matched embryos. Note the limited expansion of the lumen of the gut and disorganization of the gut epithelium in Sec13 morphants. (**B**) The intracellular organization of the ER–Golgi interface is disrupted in morphant epithelial cells. Suppression of Sec13-induced distension of the ER and accumulation of budding profiles (see insets for second example). (**C**) Sec13-depleted intestinal epithelial cells are attached to surrounding cells but a clear basal lamina (indicated by dotted lines, compare with control) is missing. (**D**) TEM of intestinal epithelial cells reveals that the microvilli seam was intact in Sec13 morphants but cell monolayer formation was disorganized, as evident from the diverse range of surface areas of the cells reaching the lumen. Total of three embryos analyzed for each oligo used. The intestinal phenotype of all of zebrafish included in this study was defined by showing pectoral fin defects as published previously (Townley et al., 2008). BL, basal lamina; E, epithelial cells; I, intestinal lining; N, nucleus. Scale bars: 0.5 μm (B,C); 1 μm (D).

Indeed, the structure of the ER and Golgi were perturbed in Sec13 morphants (Fig. 1B), consistent with a trafficking defect. The apical surface showed a developing microvilli seam in controls as well as in morphant fish, indicating that overall cell morphology was not completely disrupted. The failure to polarize epithelial cells and generate a regular gut epithelium suggested a basolateral trafficking defect. Indeed, Sec13 suppression coincided with a disrupted and reduced basal lamina in morphant embryos (Fig. 1C, compare dotted lines). Collagen IV, of which most of the basal lamina is comprised, was the most likely candidate for a transport defect. The uneven contribution of single cells to the apical surface in Sec13 morphants (Fig. 1D) further indicated compromised monolayer formation of the gut epithelium, as seen in the histological sections (Fig. 1A). This defect did not arise from gross differences in cell size (Fig. 1, compare D with E; the irregular contrasting in Fig. 1D was due to a sectioning artefact).

Sec13–Sec31 is required for epithelial morphogenesis in vitro

In order to define the mechanistic requirements for high efficiency COPII-dependent secretion we suppressed Sec13 in Caco-2 cells, a human epithelial colon cancer cell line. Because Caco-2 cells require 2 weeks to develop polarity on permeable supports and to form cysts when embedded in 3D matrix, we used lentiviral transduction to stably suppress expression of Sec13. Immunoblotting was used to confirm suppression of expression of both Sec13 and Sec31A in stable cell lines (Fig. 2A). We have previously shown that depletion of Sec13 results in concomitant suppression of Sec31A (Townley et al., 2008), resulting in highly effective reduction in the amount of the outer layer of the COPII coat. We imaged epithelial organization in polarized monolayers of control and Sec13-suppressed Caco-2 cells grown on permeable supports using confocal microscopy to view cells in X–Z view (i.e. parallel to the filter support). In control cultures, a single monolayer of cells was formed but in Sec13-depleted cells, the monolayer organization was lost, with cells growing over one another to form a multilayered sheet of cells (Fig. 2B). This disorganization was particularly obvious following 3D rendering of cell nuclei (Fig. 2C, each nucleus is shown in a different colour). Cells failed to grow as a single cell layer, with large areas of the filter showing cell layers of two, three and even four cell depths. Electron microscopy of Caco-2 monolayers showed that Sec13 suppression caused extensive disorganization of intercellular junctions with extended areas of interdigitated plasma membrane compared with control cells treated with scrambled shRNA (Fig. 2D, arrows).

We then used scanning electron microscopy (SEM) and transmission electron microscopy (TEM) to define the defects in monolayer organization of Caco-2 cells grown on permeable supports in more detail. No defects were seen in the ability of cells formation of microvilli at the apical surface following Sec13-Sec31 suppression (Fig. 3, compare B with A). Monolayer

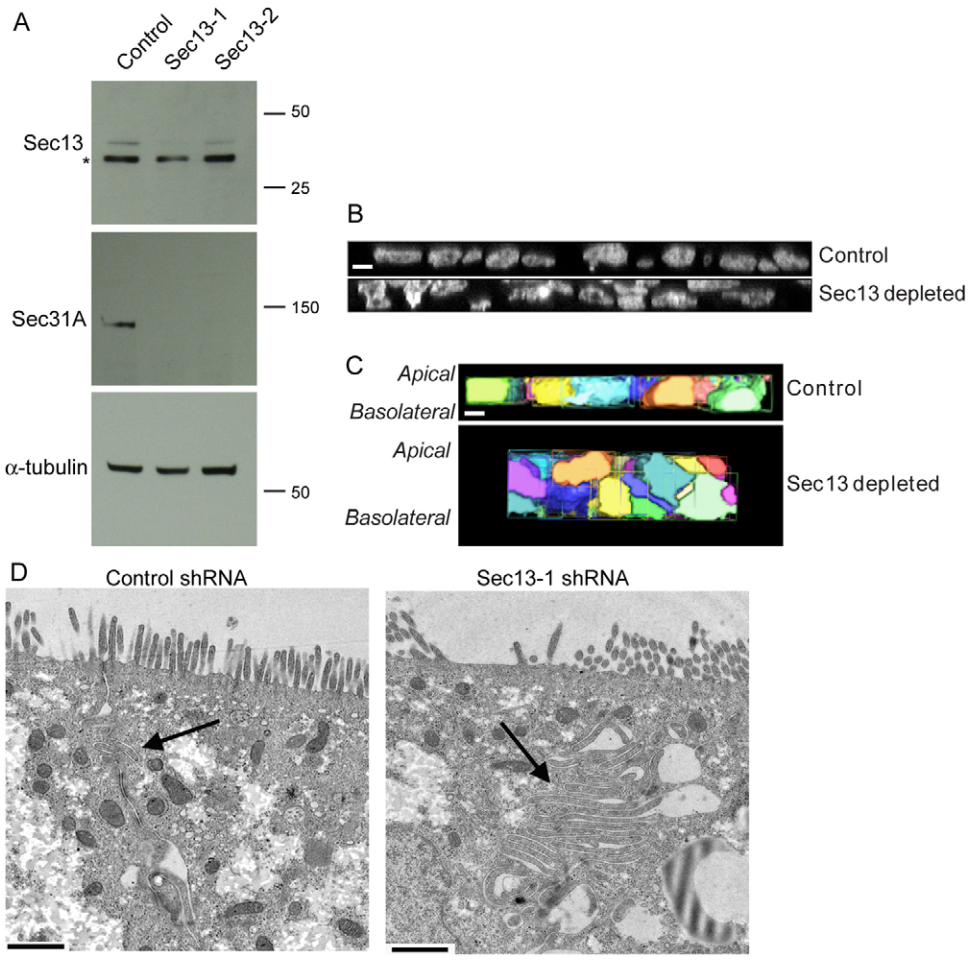

Fig. 2. Stable suppression of Sec13 expression in Caco-2 cells. (**A**) Immunoblotting of lysates from cells transduced with lentiviral constructs as indicated. Lysates of cells stably expressing shRNA were immunoblotted for Sec13, Sec31A and α-tubulin as indicated. Molecular markers are shown in kDa. The asterisk marks a nonspecific band detected by the antibody. (**B**) X–Z reconstructions of DAPI-labelled nuclei of epithelial monolayers grown for 14 days on a permeable support from control or Sec13-1 Caco-2 cells. (**C**) Automatic detection of cell nuclei and pseudo-colouring highlights the disorganization of the epithelial layer following suppression of Sec13. (**D**) TEM of polarized Caco-2 monolayer cultures from control and Sec13-1-suppressed cells. Note the extensive interdigitation of intercellular junctions on suppression of Sec13 (arrows). Scale bars: 2 μm.

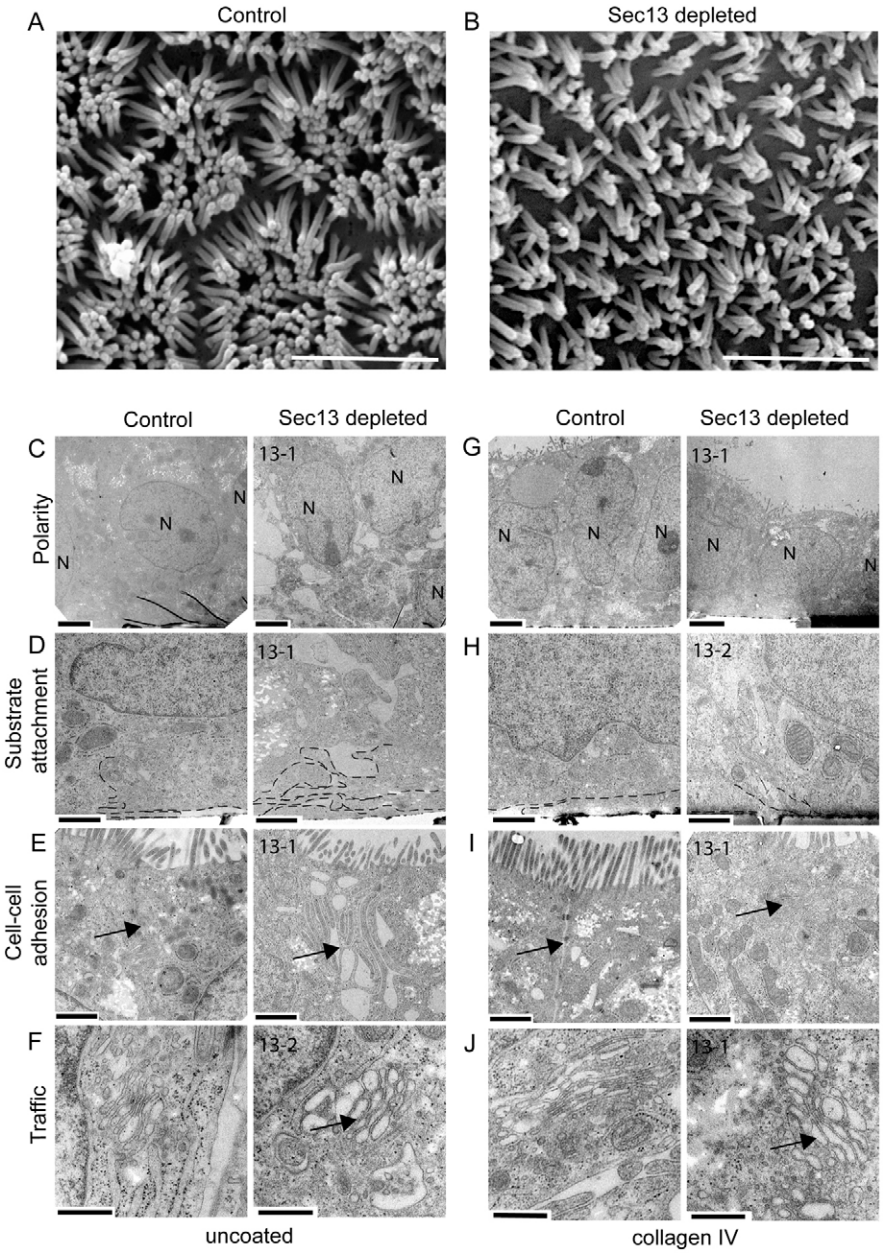

Fig. 3. Electron microscopy of epithelial organization in Sec13-depleted Caco-2 cells. (**A**,**B**) SEM of microvilli on the apical surface of Caco-2 monolayers grown for 14 days on transwell filters: (A) control cells, (B) Sec13-depleted cells. (**C–F**) Polarized Caco-2 cells stably expressing control or Sec13 shRNAs as indicated were examined for (C) polarity (i.e. the formation of monolayers), (D) attachment to the substratum (dotted lines indicate basal cell surface), (E) intercellular adhesion (cell–cell attachment indicated by arrows) and (F) ER–Golgi membrane organization. (**G–J**) Cells were also examined by TEM following growth for 14 days on collagen-IV-coated permeable supports (G, polarity; H, attachment; I, adhesion; J, ER and Golgi membrane traffic). Two independent samples were analyzed for each condition. N, nuclei. Scale bars: 2 μm (A–C); 1 μm (D,E); 0.5 μm (F).

organization was clearly affected (Fig. 3C, as seen in Fig. 2B,C). Attachment to the filter support was also reduced, as judged by the proximity of the basal membrane to the filter in electron microscopy sections (Fig. 3D, dashed lines). The intercellular junctions between cells were strongly affected by Sec13 depletion (Fig. 3E, arrows indicate the extensive gaps evident between cells depleted of Sec13), and clear defects in intracellular membrane traffic were evident (Fig. 3F, note distension of the ER, arrow). These trafficking defects recapitulate those we have described previously following depletion of Sec13 in HeLa and fibroblast cells (Townley et al., 2008). The data from Caco-2 cells showed that the situation in vitro largely resembles that in vivo.

We then sought to determine whether this phenotype could be caused cell-autonomously by a failure of the intestinal epithelial cells to secrete specific matrix components, rather than a generalized lack of ECM, which could occur in zebrafish morphants where all cells, not just intestinal epithelial cells, are suppressed for Sec13. In situ, intestinal epithelial cells grow on a basement membrane largely composed of collagen IV and laminin-1 (Timpl, 1996). The attachment to this basement membrane directs polarization and epithelial organization of intestinal cells. On the basis of our initial results we hypothesized that the defects in monolayer organization in Sec13-depleted Caco-2 cells resulted from defective ECM secretion or assembly (Townley et al., 2008; Townley and Stephens, 2009). We therefore aimed to replace the putatively incomplete ECM by coating the permeable supports with collagen IV prior to seeding cells. Caco-2 cells grown on collagen-IV-coated filters for 14 days showed marked improvements in monolayer

organization (Fig. 3G), attachment to these filters (Fig. 3H) and intercellular adhesion (Fig. 3I, arrows). Notably, no difference in terms of enlarged ER (Fig. 3J, arrow) was seen between Sec13-depleted cells grown in the presence or absence of collagen IV, indicating that the trafficking defect could not be restored by replacing a putatively missing ECM component. Our interpretation of these data is that exogenously added collagen IV improves cell–matrix adhesion and polarization of the cells and, hence, partially compensates for the failure to transport large cargo. By contrast, changes in the ER–Golgi structure and in bud formation are associated directly with the loss of Sec13-Sec31 and cannot be rescued by outside-in signalling from the ECM.

COPII-dependent secretion is essential for epithelial morphogenesis in 3D culture

Because 'rescue' of the phenotype by collagen IV alone was incomplete, we reasoned that additional secreted components are probably involved. In order to define whether ECM proteins might compensate for a secretion defect in Sec13-depleted cells, we embedded cells in 3D matrix because a complete matrix to direct polarization, polarity and organization would be provided exogenously. Engelbreth–Holm–Swarm (EHS)-tumour-derived matrix (from mice) is widely used for 3D cell culture and comprises primarily collagen IV, entactin, perlecan and laminin (Grant et al., 1985). The laminin is predominantly laminin-1, including the α1, β1 and γ1 subunits, i.e. the essential form of laminin for correct Caco-2 polarity and organization (De Arcangelis et al., 1996). Caco-2 cells form cysts when embedded in 3D EHS-derived matrix such as Matrigel or Geltrex (Ivanov et al., 2008; Jaffe et al., 2008). We anticipated that embedding Sec13-depleted cells in such matrix would support the formation of cysts indistinguishable from those of control cells.

Control cells formed spherical 3D cysts as expected (Fig. 4A, control). Apical–basolateral polarity was established and lumen expansion was evident (Ivanov et al., 2008; Jaffe et al., 2008). Comparing only cyst-like formations, the localization of polarity markers β-catenin (Fig. 4A) or epithelial-specific antigen (ESA; Fig. 4B) to the basolateral membrane was similar in both control and Sec13-suppressed cysts. Some increased lateral labelling of β-catenin was evident (Fig. 4A), as was some enhanced intracellular labelling of ESA (Fig. 4B). Assembly of filamentous actin at the apical surface was evident in all cysts formed from Sec13-suppressed cells (Fig. 4A,B). However, Sec13-suppressed cells grew into much smaller cysts with a small but significant reduction in cell number (Fig. 4C). Most obviously, Sec13-depleted cysts failed to show efficient lumen expansion (Fig. 4A,D) and indeed often failed to form any lumen at all (Fig. 4A, arrows) or formed cysts with multiple lumens (Fig. 4B, arrows). Quantification of lumen size confirmed a marked defect in lumen expansion following Sec13 suppression (Fig. 4D). Lumen expansion requires fluid filling of the interior of a cyst. Activation of protein kinase A (PKA) with N6-benzoyl-cAMP (6-Bnz-cAMP), which stimulates PKA-dependent fluid filling of the lumen (Jaffe et al., 2008) did not enhance lumen expansion of Sec13-depleted cysts. However, uniformity of the cysts was noticeably improved by addition of 6-Bnz-cAMP and so this was included in all following experiments.

We reasoned that reduced cell number within the cysts and the disorganization seen could at least in part arise through defective control of cell division. Recent data showed that depletion of Cdc42 in Caco-2 cells caused defects in cyst morphogenesis comparable to the defects seen in our experiments, which were linked to misalignment of the mitotic spindle axis during cyst expansion (Jaffe et al., 2008). It has been well documented that the ECM dictates the orientation of the spindle axis during mitosis in a variety of systems (Bornens, 2008). A significant difference in spindle alignment was seen between cysts grown from control cells and those grown from Sec13-suppressed cells (Fig. 4E, α-tubulin labelling). Sec13 suppression resulted in a significant misalignment of spindles in dividing cells grown at the periphery of cysts (i.e. the direction of cyst expansion) (Fig. 4F). We also noticed significantly more mitotic cells within the centre of cysts (Fig. 4E). This is consistent with the multi-layering of cells seen in Sec13-depleted cells grown on filters and is in agreement with a failure of signalling from the ECM to spatially direct cell division (Bornens, 2008; Jaffe et al., 2008).

ECM secretion from and deposition by Sec13-suppressed cells

Our data show that exogenously supplied ECM is necessary to direct polarization and the initial stages of cyst formation in 3D of Sec13-suppressed Caco-2 cells. Because supplying collagen-IV-rich matrix was not sufficient to complete cyst lumen expansion, our data suggested that on-going cell autonomous secretion is required to finalize cyst polarity and organization. The defects in morphogenesis could result from a defect in secretion of ECM components that are not supplied by EHS-derived matrix, or from a failure to secrete small, soluble factors.

Our working hypothesis was that Sec13 depletion leads to a defect in deposition of large ECM components such as collagen (Townley et al., 2008), therefore we went on to monitor the secretion of these macromolecules, initially in 2D cultures. We used immunofluorescence of ECM deposited by Caco-2 cells grown on glass coverslips (following removal of cells). These experiments showed that Sec13 suppression resulted in reduced deposition of collagen I and perlecan (Fig. 5A,B). In 3D culture, collagen IV secretion and/or remodelling was not significantly different in control and Sec13-depleted cells (Fig. 5C). The antibody used was not human-specific and therefore these data reflect the ability of Sec13-depleted cysts to assemble collagen IV derived from the supplied mouse 3D matrix. Cells depleted of Sec13 also showed a reduction in assembly of laminin-1 compared with controls when grown in 3D culture (Fig. 5C,D). The antibody used also detects laminin-1 from EHS-derived matrix and so these data could reflect either an inability of Sec13-depleted cells to secrete laminin-1, or a failure of cysts to organize the surrounding laminin network. Immunoblotting of cell-derived matrix (i.e. that remaining following removal of cells from the culture dish) with antibodies to different laminin subunits showed a surprising increase in laminin secretion by Sec13-depleted cells (Fig. 5E), demonstrating that the defects seen in Fig. 5C resulted from a failure to organize the laminin matrix rather than a failure to secrete laminin. Using 2D gel electrophoresis of proteins <50 kDa, we could not detect any differences in the soluble secretome of control or Sec13-suppressed Caco-2 cells (supplementary material Fig. S1A,B). This was consistent with the lack of detectable defects in the transport or secretion of small, soluble, freely diffusible proteins or transmembrane proteins in Sec13-suppressed HeLa cells (Townley et al., 2008) and Caco-2 cells (gp135/podocalyxin;

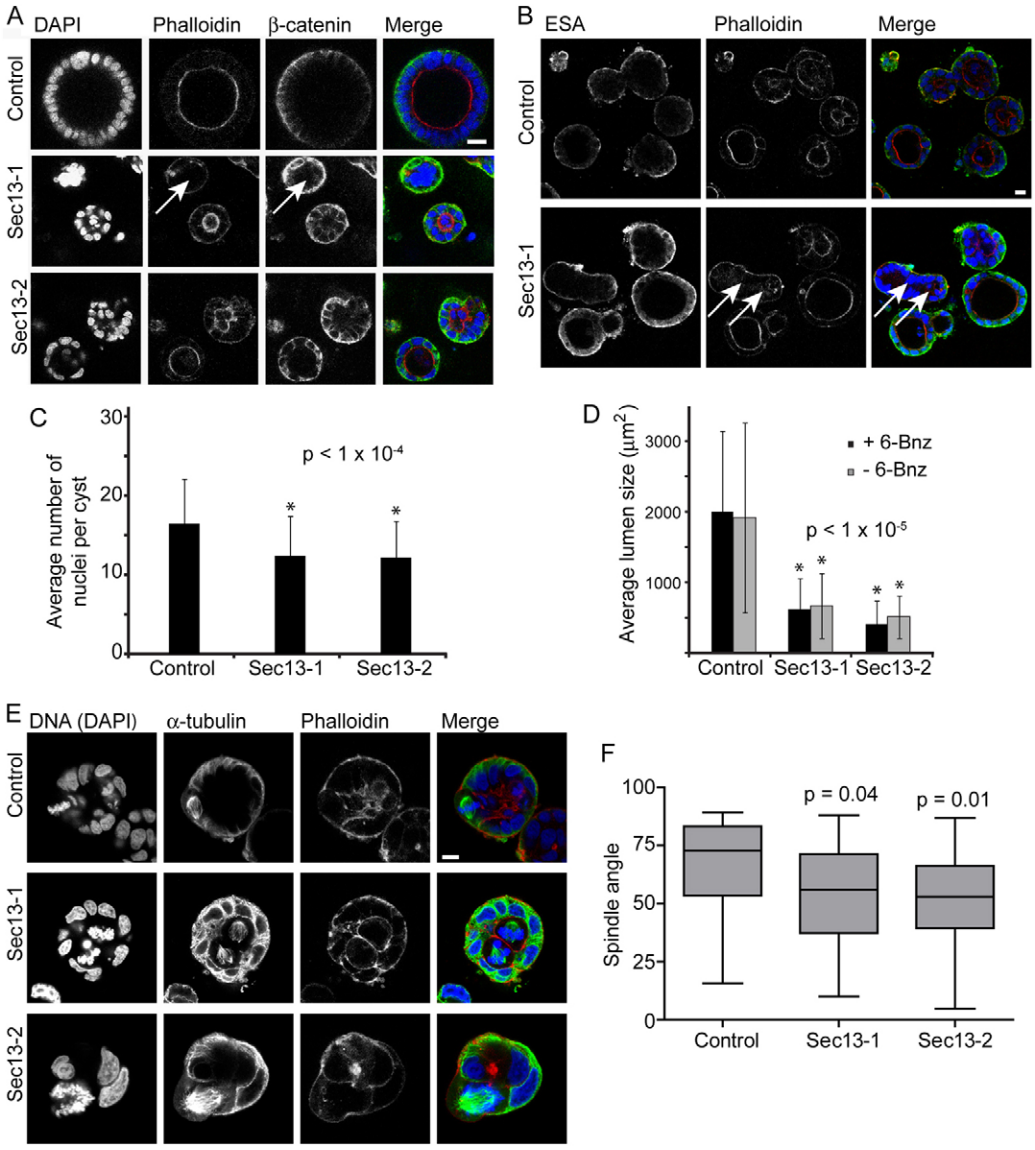

Fig. 4. Sec13 suppression disrupts cyst formation by Caco-2 cells embedded in 3D matrix. (**A**) Formation of cysts by Caco-2 cells grown for 7 days in 3D matrix is inhibited by Sec13 suppression. Organization of the cell monolayer is affected compared with controls (DAPI labelling of nuclei), as is expansion of the central lumen (highlighted by phalloidin labelling of filamentous actin). Cysts are also smaller. (**B**) Basolateral targeting is unaffected as shown by labelling for ESA. (**C**) The number of cells per cyst is also decreased, indicating a cell division defect. (**D**) Quantification shows that lumen size (lumen area at the point of maximum cyst width) is significantly decreased on Sec13 suppression (with or without the presence of 6-Bnz). In A–D, $n>40$ cysts in each of three independent experiments performed for each experimental condition. Error bars represent s.e.m. *P* values compare depleted samples with control. (**E**) Alignment of the mitotic spindle (tubulin labelling) is perturbed in Sec13-depleted cysts, with frequent mitotic profiles seen in the centre of cysts as well as in the limiting layer. (**F**) Quantification of spindle alignment in these cysts. Median values are shown by the horizontal bar within each box; boxes show 25th and 75th percentiles; whiskers show the spread of the data. In E and F, $n=30$ cysts for each shRNA from three independent experiments. Scale bars: 20 μm.

data not shown). However, we cannot rule out defects in small cargo secretion that are undetectable using this approach.

Rescue of cyst lumen expansion by co-culture with fibroblasts

EHS-derived matrix largely lacks fibrillar collagens (Grant et al., 1985). Because we found that COPII-dependent secretion of collagen I is impaired on Sec13 suppression (Townley et al., 2008) (and this study), we sought to define whether exogenous collagen type I could rescue lumen expansion in 3D culture. Adding soluble collagen I to EHS-derived matrix directly did not improve cyst morphogenesis, but this was probably due to improper fibril assembly of the purified rat tail protein used. Our data pointed towards a missing secreted factor that is required for cyst formation. We chose to determine whether this could be provided exogenously by co-culturing Sec13-depleted Caco-2 cells with normal human fibroblasts. We incorporated an equal number of primary human fibroblasts into the 3D culture (Fig. 6A). In these experiments, control cells grew well and developed into 3D cysts with fully expanded lumens (Fig. 6A). Notably, in the presence of fibroblasts, Sec13-depleted cells also grew into large cysts with enhanced lumen expansion compared

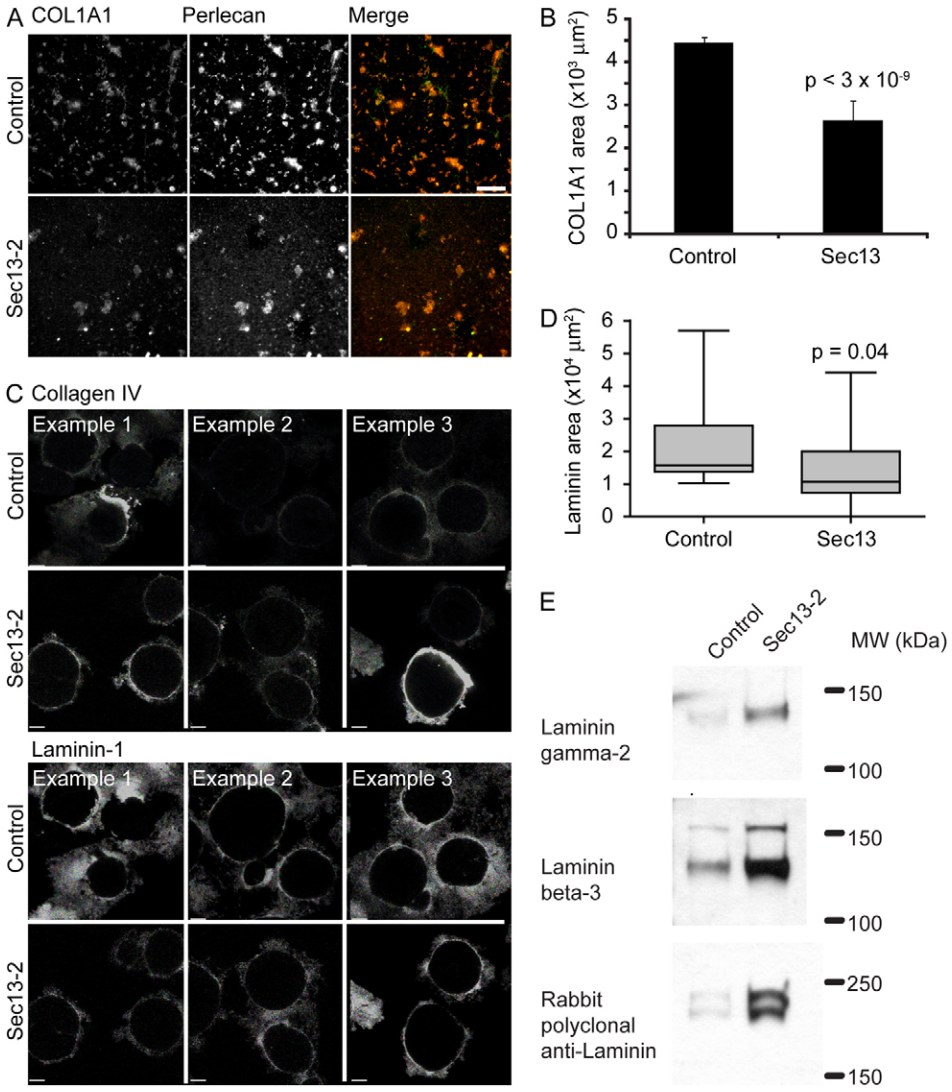

Fig. 5. Deposition and assembly of ECM surrounding epithelial cysts is impaired following Sec13 depletion. (**A**,**B**) Collagen I and perlecan deposition by cells grown on glass coverslips was analyzed by immunofluorescence microscopy following removal of cells. B shows quantification of results. (**C**,**D**) Collagen IV assembly around epithelial cysts grown in 3D matrix is unaffected by Sec13 suppression. By contrast, laminin-1 labelling around control cysts covers a much greater area than that surrounding cysts formed from Sec13-depleted cells. The intensity of labelling immediately surrounding the cyst is also significantly reduced following Sec13 suppression. Three examples are shown in C. Quantification of laminin labelling is shown in D. Median values are shown by the horizontal bar within each box; boxes show 25th and 75th percentiles; whiskers show the spread of the data. n=26 cysts total from three independent experiments. (**E**) Immunoblotting of cell-derived matrices. Cells were grown for 10 days in tissue culture dishes with ascorbic acid feeding. Cells were denuded and the remaining matrix was removed and added to sample buffer. Samples were immunoblotted with the following antibodies: laminin γ-2, laminin β-3 and rabbit polyclonal antibody against laminin (which recognises A chain, B1 chain and B2 chain). Molecular mass is indicated in KDa. Scale bars: 20 µm.

with controls (Fig. 6A,B). This increase in cyst size resulted from an increase in cell number per cyst rather than cell size. We observed that the fibroblasts grew as a layer below the cysts and hence were not visible in the confocal sections shown. We then used conditioned medium from fibroblasts to define whether a soluble secreted factor would be sufficient to rescue the cyst expansion defect seen on Sec13 depletion. Fig. 7 shows that addition of medium from normal dermal fibroblast (NDF) cultures had no significant effect on growth of control cysts (Fig. 7, compare B with A) and can partially rescue lumen formation in Sec13-depleted cysts (Fig. 7, compare D with C). These data were quantified and average lumen sizes (for those cysts with any lumen expansion) are shown schematically in Fig. 7E–H and graphically in Fig. 7I. We sought to define whether this soluble secreted factor might be collagen I by stably depleting collagen type I α1 (COL1A1) from fibroblasts. However, all fibroblasts transduced with virus to deplete COL1A1 did not survive in culture, even when grown on a thin coating of Getrex.

Discussion

We have shown here that Sec13 depletion results in defects of epithelial morphogenesis in vivo and in vitro. We can largely rescue epithelial monolayer formation in 2D transwell cultures by addition of collagen IV. In 3D culture, a collagen-IV-rich matrix is not sufficient to drive full lumen expansion in 3D. These data highlight the requirement for efficient COPII-dependent secretion in cyst morphogenesis in vitro. We can substantially restore cyst generation of Sec13-depleted Caco-2 cells by adding fibroblasts, or indeed conditioned medium from fibroblasts, to our 3D culture system. In both cases, however, the rescue was incomplete. It can therefore not be excluded that COPII-dependent export from the ER is required to organize intracellular signalling pathways to direct epithelial morphogenesis, or that this can be a contributing factor. Equally, it is possible that the export of one or more small soluble factors is disturbed such that cyst formation is impaired. However, our data suggest that this might be unlikely; 2D gel electrophoresis of the secreted proteome of Sec13-suppressed Caco-2 cells (supplementary material Fig. S1) revealed no differences in the secretion of small soluble cargo, similarly to previous work in HeLa cells (Townley et al., 2008). These data are consistent with the hypothesis that a stabilized COPII coat is required to direct ER export of large and bulky cargo such as ECM components (Townley et al., 2008; Schmidt and Stephens, 2010) but do not rule out a requirement for the secretion of non-ECM cargoes of any size.

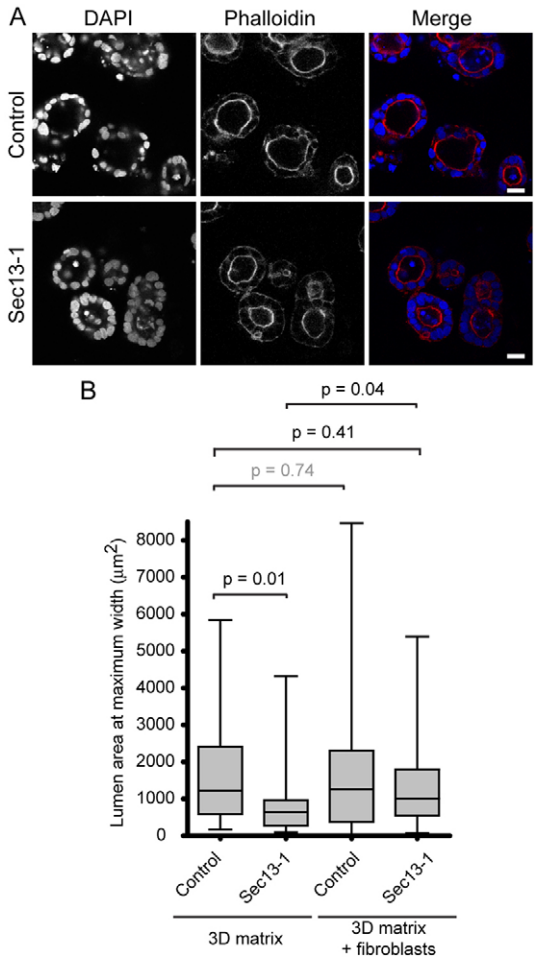

Fig. 6. Cyst morphogenesis defects in 3D matrix following Sec13 suppression can be substantially rescued by co-culture with human fibroblasts. (**A**) Lumen formation is partially restored in cysts formed from Sec13-suppressed cells in the presence of fibroblasts. Cysts are more spherical, showing well-defined apical actin organization. Cells are still seen within the cyst in addition to the limiting monolayer, suggesting a partial but incomplete recovery of morphogenesis. Scale bar: 20 µm. (**B**) Quantification of cyst lumen area from three independent experiments shows that growth in the presence of fibroblasts restored lumen expansion to Sec13-1 depleted cysts. Similar results were obtained for Sec13-2 cells. Boxes show the median with 25th and 75th percentiles; whiskers show the spread of the data. n>20 (typically 20–30) cysts in each of three independent experiments performed for each experimental condition. Results of statistical testing (Student's t-test) compared with controls in 3D matrix alone are indicated.

Because normal ER morphology was not restored by supplementing the ECM with fibroblasts, impaired COPII budding at the ER following Sec13 suppression does not appear to result from a failure of ECM-dependent outside-in signalling. We favour a model based on a selective defect in secretion and assembly of ECM. Attempts to test the requirement for COL1A1 secretion by fibroblasts in our co-culture system were not possible. COL1A1 suppression in fibroblasts resulted in loss of adhesion to plastic dishes and, consequently, we were unable to amplify these cells for co-culture with Sec13-depleted Caco-2 cells.

Although our data show that ECM secretion is dependent on the outer layer of the COPII coat, they do not preclude the possibility that ECM export from the ER, although COPII-dependent, might not in fact occur in COPII-coated carriers (Mironov et al., 2003). Such a model implies that the role of COPII is in trafficking of accessory factors that are required for cargo export, such as tethers and SNAREs. Our current favoured model is that Sec13–Sec31 encapsulates nascent vesicle buds containing fibrillar collagen and large cargo as they emerge from the ER (Stagg et al., 2008; Schmidt and Stephens, 2010). Our data are consistent with models in which reduced Sec13–Sec31 causes a failure to scaffold the formation of such carriers. Notably, recent data have shown that Sec13–Sec31 can form tubular structures in vitro that might serve as containers for fibrillar collagen in vivo (O'Donnell et al., 2010). Whether this occurs via a receptor-mediated mechanism as has been proposed for TANGO1-mediated export of collagen (Saito et al., 2009; Wilson et al., 2011), or simply due to a geometric requirement for ordered Sec13–Sec31 assembly around larger export containers (Stagg et al., 2008), or even a combination of the two, is a question for future research. In further support of the notion of encapsulation of collagen within a COPII-coated carrier, Aridor and colleagues showed recently that a mutant form of Sar1 (with key substitutions in a conserved C-terminal loop) did not affect recruitment of other COPII proteins, nor Sar1 activation, but did inhibit oligomerization of Sar1 and type I procollagen export from the ER (Long et al., 2010). The authors propose that deregulation of membrane constriction is responsible, such that the mutant form of Sar1 indirectly prevents entry of procollagen into Sar1-coated tubules.

A dynamic interplay between both epithelial and surrounding cells in terms of ECM deposition and remodelling is certainly necessary to direct morphogenesis in vivo (Kedinger et al., 1998; Simon-Assmann et al., 1998; O'Brien et al., 2001; Martin-Belmonte et al., 2008). The difference in ECM composition surrounding Sec13-depleted cysts could be either due to a selective defect in secretion, or impaired matrix assembly. Our observation that laminin-1 assembly around Sec13-suppressed cysts is impaired points to an additional defect in matrix remodelling. Rac1-dependent remodelling of the laminin network has been shown to be essential for cyst morphogenesis in other systems (O'Brien et al., 2001). It is also possible that the defect in Sec13–Sec31 coupling reduces secretion of other key macromolecules (or molecules) that are required but not involved in ECM assembly.

We also found perlecan levels to be reduced and this could contribute to the phenotype because perlecan crosslinks several matrix components and, hence, is likely to be involved in collagen and/or laminin assembly in Sec13-depleted cysts. However, if knockdown of Sec13 in zebrafish results in a general defect of perlecan secretion one would expect to largely reproduce the phenotype of a knockout of perlecan in mice (Rossi et al., 2003). For example, knockout of perlecan was reported to have a major affect on the lens capsule and we never observed any effects on lens integrity in Sec13 morphants (Townley et al., 2008) (K.S. and D.J.S., unpublished observations). We therefore assume that a defect of perlecan secretion is unlikely to play a major causative part in the failure of tube formation in Sec13-depleted Caco-2 cells.

It has been well documented that the ECM dictates the orientation of the spindle axis during mitosis in a variety of systems (Bornens, 2008). Caco-2 cyst morphogenesis requires Cdc42-dependent signalling to specify the alignment of the mitotic

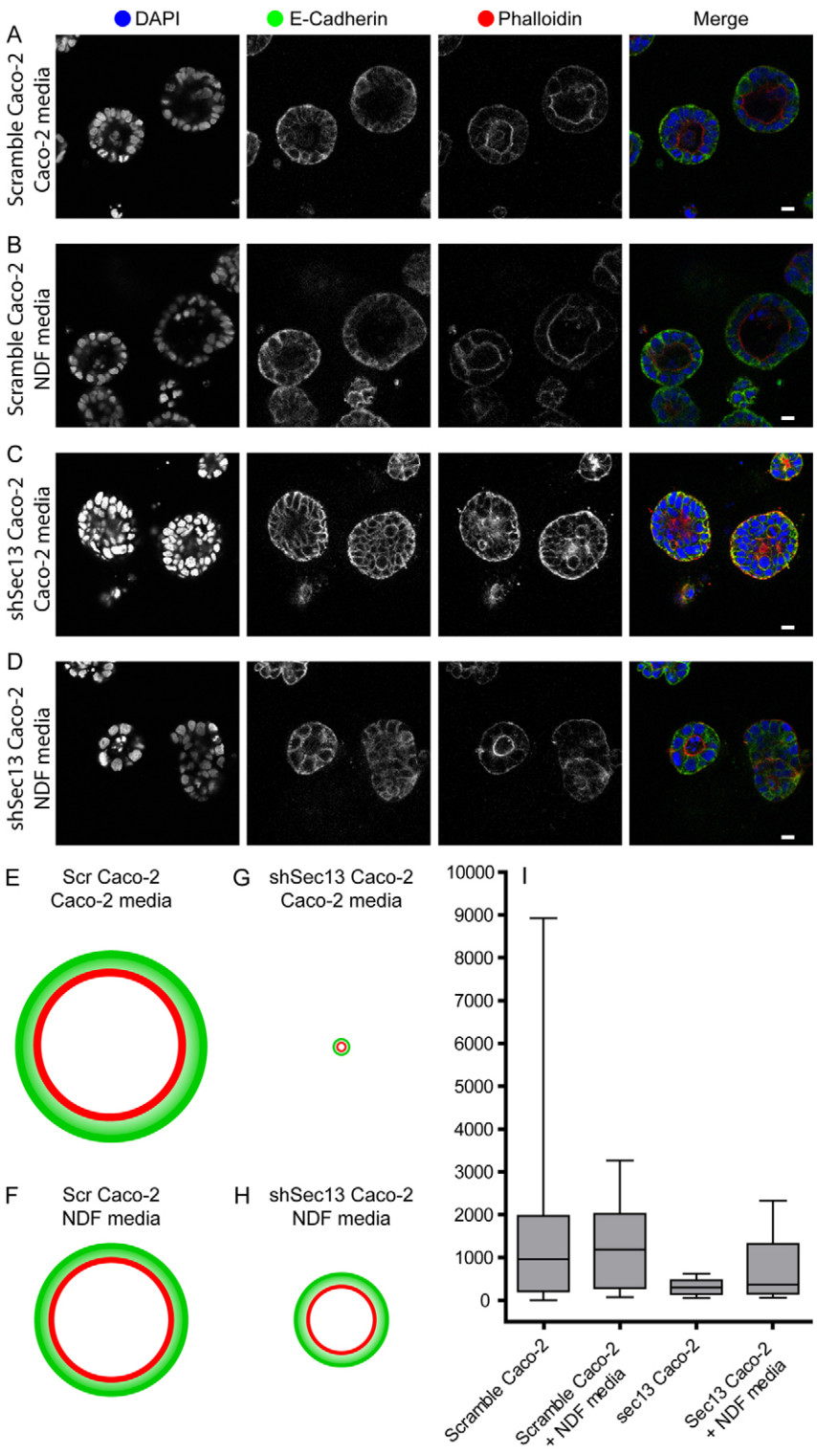

Fig. 7. Rescue of Sec13 lumen defect by addition of fibroblast-conditioned medium. Caco-2 cells expressing scrambled shRNA or Sec13 shRNA were embedded in Geltrex and grown for 7 days. Cells were grown in the presence of either control (Caco-2) medium or conditioned medium taken from a confluent dish of NDF. (**A**) Scramble shRNA-transfected Caco-2 cells plus Caco-2 medium. (**B**) Scramble shRNA-transfected Caco-2 cells plus NDF medium. (**C**) Sec13 shRNA-transfected Caco-2 cells plus Caco-2 medium. (**D**) Sec13 shRNA-transfected Caco-2 cells plus NDF medium. (**E–H**) Representation of mean lumen area for cysts formed in A–D; green represents basolateral surface with the apical surface in red. (**I**) Quantification of mean lumen size for cysts in A–D; median values are shown by the horizontal bar within each box; boxes show 25th and 75th percentiles; whiskers show the spread of the data. n>20 cysts in each of three independent experiments performed for each experimental condition. Scale bars: 10 µm.

spindle and this results in subsequent positioning of the apical surface during cyst expansion (Jaffe et al., 2008). We noticed a significant misalignment of mitotic spindles in cysts grown from Sec13-suppressed cells. Our interpretation of the data is that COPII-dependent secretion (including secretion of ECM components) and subsequent remodelling of laminin-rich ECM is secondarily required for Cdc42 activation, consistent with work showing that outside-in signalling by laminin-1 is required for Cdc42 activation in neurite outgrowth (Weston et al., 2000).

Caco-2 cells (and other epithelial lines) in both 2D and 3D culture are widely used in basic biomedical science but also in the pharmaceutical industry. An important outcome of these experiments is the demonstration that epithelial cells, when embedded in a 3D matrix, retain an essential requirement for

COPII-dependent secretion in order to fully differentiate into an epithelial cyst. Given the conservation of membrane trafficking between species, this is likely to be true for other widely used model systems, including Madin-Darby canine kidney cells and mouse mammary gland epithelia. The necessity for ongoing secretion by Caco-2 cells in 3D culture has key implications for the interpretation of any work using 3D cell culture models. Our data show that exogenously supplied EHS-derived matrix alone is not sufficient to facilitate proper cyst morphogenesis. Experimental outcomes that show clear defects in epithelial organization and morphogenesis could result from secondarily impaired ECM secretion rather than only from primary effects on intracellular signalling pathways. Taken together, the data we present here show that efficient COPII assembly and function is indispensable for completion of epithelial and cyst morphogenesis. The exact nature of late COPII function and potentially affected cargo molecules will require further research. Our results have significant implications for COPII function, for epithelial polarity and organization in vivo, and for the interpretation of experiments using Caco-2 cells embedded in EHS-derived tumour matrix.

Materials and Methods

All reagents were purchased from Sigma-Aldrich (Poole, UK) unless otherwise indicated.

Growth of cultured cells.

Caco-2 cells were maintained in DMEM supplemented with 10% FCS (Invitrogen, Paisley, UK), 1% glutamine and 1% non-essential amino acids. Primary human dermal fibroblasts were purchased from Cascade Biologics (Invitrogen) and were cultured in Medium 106 supplemented with low-serum growth supplement. At 24 hours prior to the start of the experiments, cells were seeded onto either 22-mm coverslips, glass-bottom dishes (MatTek, Ashland, MA) or polyester transwell permeable supports (Corning).

Antibodies and other reagents

Monoclonal mouse anti-human collagen IV (MAB1910, anti-collagen type IV α2 chain, clone 23IIC3) was from Millipore (Watford, UK); polyclonal anti-laminin (ab11575) was from Abcam (Cambridge, UK); and rat monoclonal anti-heparan sulphate proteoglycan (Perlecan, MAB1948, clone number A7L6) was from Millipore. The following antibodies were used to detect laminin: laminin γ2 (SC-7652; Santa Cruz Biotechnology, Santa Cruz, CA), laminin β3 (SC-20775; Santa Cruz Biotechnology) and rabbit polyclonal to laminin (which recognises A chain, B1 chain and B2 chain) (ab11575; Abcam, Cambridge, UK). Anti-β-catenin (C19220-050, clone number 14) was from BD Transduction Laboratories (Franklin Lakes, NJ). Anti-tubulin (MS-581-P0, clone DM1A) was from Neomarkers (Fremont, CA). Sec13 antibodies were a generous gift from Wanjin Hong (IMCB, Singapore) and Beatriz Fontoura (Southwestern Medical Center, Dallas, TX). Anti-gp135/podocalyxin was kindly provided by Paul Verkade (University of Bristol, Bristol, UK). Anti-Sec31A antibodies were raised against synthetic peptides synthesized by Graham Bloomberg, University of Bristol and coupled to KLH before immunization into rabbits. Antibodies were affinity purified using peptide coupled to sulfolink resin (Pierce, Cramlington, UK) using the manufacturer's protocols. The peptide sequence was MKLKEVRTAMQAWS(C), C-terminal cysteines were added for coupling. Mouse monoclonal ESA was a kind gift from André Le Bivic (IBDM, Marseilles, France). Secondary antibodies were from Jackson ImmunoResearch Laboratories (West Grove, PA). Alexa-Fluor-568-labelled phalloidin was from Molecular Probes.

Lentiviral constructs and generation of stably suppressed cell lines

Short hairpin RNA (shRNA) lentiviral particles were from Dharmacon (Thermo Scientific). The sequences targeted were 5′-GCCTTAACGTGATCGGAGA-3′ for Sec13-1 and 5′-ATGAGGACATGATTCACGA-3′ for Sec13-2. Caco-2 cells were plated at 1.5×10^5 cells per 3-cm tissue culture dish and infected with lentivirus particles according to the manufacturers' instructions. Following puromycin selection, stable cell lines were verified by western blot and immunofluorescence. Controls were infected with a scrambled shRNA lentivirus.

Growth of Caco-2 cells in 2D and 3D

Caco-2 stable cell lines were grown on permeable supports to allow polarization. Polyester transwell permeable supports, 0.4 μm thick and 12 mm diameter were from Corning. Cells were seeded at a density of 2×10^5 cells per insert and cultured for 2 weeks with media changes every other day. The cells were then either processed for immunofluorescence or electron microscopy. For growth in 3D, stable cell lines were seeded into Geltrex (Invitrogen) to allow polarization into 3D cysts. All experiments shown were performed using a single lot number. Cells were trypsinized and counted, and then 6×10^4 cells per well in an eight-well chamber slide were mixed with Geltrex to give a final concentration of 40%. A sample of 100 μl was plated into the chamber slide well and incubated at 37℃ for 30 minutes to allow the Geltrex to solidify. Fresh medium (400 μl) was then added on top. Cells were cultured for 3 days or 7 days with media changes every other day.

Cell-derived matrices

Culture dishes were prepared before seeding with live cells by first washing with phosphate-buffered saline (PBS) and incubating with 0.2% sterile gelatin for 60 minutes at 37℃ (2% gelatin, Sigma G1393, diluted in PBS). They were then washed three times with PBS and crosslinked with 1% sterile glutaraldehyde in PBS for 30 minutes at room temperature. The dishes were washed three times with PBS before quenching the crosslinker with 1 M sterile glycine in PBS for 20 minutes at room temperature. The dishes were then washed three times with PBS, followed by incubation with DMEM growth medium for 30 minutes at 37℃. Caco-2 cells were trypsinized and counted using a hemocytometer; 1×10^5 cells/ml were plated and 2 ml was used per live cell dish. Cells were cultured at 37℃, 5% CO_2 overnight on the gelatin-coated dishes. The cells must be confluent throughout the generation of the matrix so, once confluent, the cells were fed with complete medium supplemented with 50 μg/ml ascorbic acid. The cells were cultured for 8 days with media changes every day using medium supplemented with 50 μg/ml ascorbic acid. To denude the cells, the medium was first removed and cells washed with PBS. Then, 1.5 ml of pre-warmed extraction buffer (20 mM NH_4OH and 0.5% Triton X-100 in PBS) was gently added. Cells were lysed for 2 minutes until no intact cells were visible. The extraction buffer was aspirated and washed twice with PBS containing calcium and magnesium. DNA residue was digested by incubating with 10 μg/ml DNase I in PBS containing calcium and magnesium for 30 minutes at 37℃, 5% CO_2. This was removed and the dishes were washed with PBS containing calcium and magnesium. The matrices were then processed for immunofluorescence or immunoblotting. For immunofluorescence, labelling with collagen IV or laminin antibodies was carried out for 2 hours at 37℃, 5% CO_2, before fixation. Other primary antibodies were incubated for 2 hours at room temperature after fixation with paraformaldehyde. For immunoblotting, matrix was solubilized in SDS-PAGE sample buffer prior to electrophoresis and immunoblotting with antibodies.

Co-culturing Caco-2 cells with normal dermal fibroblasts

Stable Caco-2 cell lines were seeded with normal human fibroblasts into Geltrex to try to rescue the lumen expansion defect. Caco-2 cells and fibroblasts were trypsinized and counted, and then 6×10^4 Caco-2 cells and 3×10^4 fibroblasts per well of an eight-well chamber slide were mixed with Geltrex to give a final concentration of 40%. Then, 100 μl was plated into each well and put at 37℃ for the Geltrex to solidify; 400 μl of Caco-2 medium was then put on top. For the conditioned medium experiment, 200 μl of Caco-2 medium and 200 μl of medium taken from a confluent dish of normal dermal fibroblasts was added. Medium was changed every 2 days and the cells were grown for 7 days to allow the formation of cysts.

Danio rerio morpholino oligonucleotide microinjection

Husbandry of zebrafish (*D. rerio*) AB strain and morpholino injection of was performed as described previously (Townley et al., 2008). Two translation-blocking morpholino oligonucleotides (Sec13-1 and Sec13-2) were validated previously (Townley et al., 2008) but for the experiments presented in Fig. 1 only that targeting Sec13-2 was used.

Electron microscopy

Sec13- or lamin-A/C (control)-suppressed Caco-2 cells were fixed in 2.5% glutaraldehyde containing 0.1 M cacodylate for 2 hours before transwell filters were cut. Morpholino-injected fish (5 dpf, days post fertilization) were fixed in 5% glutaraldehyde, 0.05 M cacodylate, 1% paraformaldehyde, 1% sucrose and 1 mM $MgCl_2$ for 2 hours. Samples were post-fixed in 1% (for cells) or 2% (for zebrafish embryos) OsO_4, respectively, and dehydrated through a graded series of ethanol. Zebrafish and cells were infiltrated with Epon and eventually embedded in moulds. The Epon was hardened for 48 hours and 50 nm sections were counterstained and analyzed with a FEI Tecnai12 Biotwin equipped with a bottom-mount 4K EAGLE CCD camera. For histology, 1 μm Epon sections of fish from the same anterior–posterior region were counterstained with Methylene Blue, mounted and imaged on a Zeiss Axioplan 2 microscope with a Qimaging digital camera.

For SEM, shRNA-expressing Caco-2 cells were fixed in 2.5% glutaraldehyde containing 0.1 M cacodylate, then post-fixed in 1% OsO_4 in cacodylate for 1 hour, dehydrated in graded ethanol, and critical-point dried (100% ethanol, carbon dioxide). The specimens were sputter-coated with gold (Edwards Sputter Coater) and viewed on a FEI Quanta4000 scanning electron microscope.

Immunolabelling

Medium was removed from the cysts and they were subsequently washed with PBS. Cysts were then fixed using 4% paraformaldehyde, for 30 minutes at room temperature. This was removed and the cysts incubated with 0.5% Triton X-100 in PBS for 30 minutes at room temperature. This was followed by incubation at room temperature with 100 mM glycine in PBS for 10 minutes. Cysts were then blocked using 3% bovine serum albumin (BSA) in PBS for 1 hour at room temperature. Primary antibodies were then incubated with the cysts overnight at 4˚C. Primary antibodies were diluted to between 1:100 and 1:200 in 3% BSA in PBS. Following incubation with primary antibodies, cysts were washed with PBS for 5 minutes and this was repeated three times. Secondary antibodies, diluted in 3% BSA in PBS, were then added and incubated for 2 hours at room temperature. Cysts were washed in PBS for 10 minutes and this was repeated three times. Nuclear staining was achieved by counterstaining cysts with DAPI for 15 minutes at room temperature. Cysts were then washed in PBS and then stored in PBS at 4˚C until they were imaged.

Confocal imaging

Cysts cultured in chamber slides and processed for immunofluorescence were imaged using a Leica AOBS SP2 confocal imaging system attached to a Leica DMIRE2 inverted microscope (Leica Microsystems, Milton Keynes, UK). Confocal Z slices of 0.8 µm were taken through the cyst using a 405 nm diode laser, a 488 nm argon laser, and 543 nm and 633 nm red HeNe lasers. Data was processed using Volocity software (Perkin Elmer) and Adobe Illustrator CS (Adobe).

Quantification of image data and statistical analysis

Analysis of spindle angle was performed as described (Jaffe et al., 2008). Analysis of lumen size and number of nuclei was performed using the measurement tools in Volocity 5.1 (Perkin Elmer). Intensity and area measurements for ECM were compared using automated object identification and counting using Volocity 5.1. Samples were compared using a Student's 1-tailed unpaired *t*-test using GraphPad Prism. Note that graphs show box and whisker plots from GraphPad, where boxes indicate the 25th and 75th percentiles and the whiskers display the spread of the data.

Acknowledgements

The authors wish to thank Harry Mellor, Mark Bass, Paul Martin, Paul Verkade and Jo Adams for very helpful discussions and critical reading of the manuscript. We acknowledge the kind gifts of antibodies from André le Bivic and Paul Verkade, and thank Yi Feng and Paul Martin for help with the zebrafish work, and Ginny Tilly for assistance with electron microscopy. We are also indebted to Kate Heesom for performing 2D gel electrophoresis.

Funding

This work was funded through an MRC Non-Clinical Senior Fellowship to D.J.S. [grant number G117/553] and a BBSRC grant [grant number E019633]. Deposited in PMC for release after 6 months.

Supplementary material available online at
http://jcs.biologists.org/lookup/suppl/doi:10.1242/jcs.091355/-/DC1

References

Abrams, E. W. and Andrew, D. J. (2005). CrebA regulates secretory activity in the Drosophila salivary gland and epidermis. *Development* **132**, 2743-2758.

Antonny, B., Madden, D., Hamamoto, S., Orci, L. and Schekman, R. (2001). Dynamics of the COPII coat with GTP and stable analogues. *Nat. Cell Biol.* **3**, 531-537.

Antonny, B., Gounon, P., Schekman, R. and Orci, L. (2003). Self-assembly of minimal COPII cages. *EMBO Rep.* **4**, 419-424.

Aridor, M., Bannykh, S. I., Rowe, T. and Balch, W. E. (1999). Cargo can modulate COPII vesicle formation from the endoplasmic reticulum. *J. Biol. Chem.* **274**, 4389-4399.

Barlowe, C., Orci, L., Yeung, T., Hosobuchi, M., Hamamoto, S., Salama, N., Rexach, M. F., Ravazzola, M., Amherdt, M. and Schekman, R. (1994). COPII: a membrane coat formed by Sec proteins that drive vesicle budding from the endoplasmic reticulum. *Cell* **77**, 895-907.

Beck, K., Hunter, I. and Engel, J. (1990). Structure and function of laminin: anatomy of a multidomain glycoprotein. *FASEB J.* **4**, 148-160.

Bi, X., Mancias, J. D. and Goldberg, J. (2007). Insights into COPII coat nucleation from the structure of Sec23*Sar1 complexed with the active fragment of Sec31. *Dev. Cell* **13**, 635-645.

Bornens, M. (2008). Organelle positioning and cell polarity. *Nat. Rev. Mol. Cell Biol.* **9**, 874-886.

Boyadjiev, S. A., Fromme, J. C., Ben, J., Chong, S. S., Nauta, C., Hur, D. J., Zhang, G., Hamamoto, S., Schekman, R., Ravazzola, M. et al. (2006). Cranio-lenticulo-sutural dysplasia is caused by a SEC23A mutation leading to abnormal endoplasmic-reticulum-to-Golgi trafficking. *Nat. Genet.* **38**, 1192-1197.

Bryant, D. M. and Mostov, K. E. (2008). From cells to organs: building polarized tissue. *Nat. Rev. Mol. Cell Biol.* **9**, 887-901.

Canty, E. G. and Kadler, K. E. (2005). Procollagen trafficking, processing and fibrillogenesis. *J. Cell Sci.* **118**, 1341-1353.

d'Enfert, C., Wuestehube, L. J., Lila, T. and Schekman, R. (1991). Sec12p-dependent membrane binding of the small GTP-binding protein Sar1p promotes formation of transport vesicles from the ER. *J. Cell Biol.* **114**, 663-670.

De Arcangelis, A., Neuville, P., Boukamel, R., Lefebvre, O., Kedinger, M. and Simon-Assmann, P. (1996). Inhibition of laminin alpha 1-chain expression leads to alteration of basement membrane assembly and cell differentiation. *J. Cell Biol.* **133**, 417-430.

Farach-Carson, M. C. and Carson, D. D. (2007). Perlecan – a multifunctional extracellular proteoglycan scaffold. *Glycobiology* **17**, 897-905.

Forster, D., Armbruster, K. and Luschnig, S. (2010). Sec24-dependent secretion drives cell-autonomous expansion of tracheal tubes in Drosophila. *Curr. Biol.* **20**, 62-68.

Fromme, J. C. and Schekman, R. (2005). COPII-coated vesicles: flexible enough for large cargo? *Curr. Opin. Cell Biol.* **17**, 345-352.

Fromme, J. C., Ravazzola, M., Hamamoto, S., Al-Balwi, M., Eyaid, W., Boyadjiev, S. A., Cosson, P., Schekman, R. and Orci, L. (2007). The genetic basis of a craniofacial disease provides insight into COPII coat assembly. *Dev. Cell* **13**, 623-634.

Grant, D. S., Kleinman, H. K., Leblond, C. P., Inoue, S., Chung, A. E. and Martin, G. R. (1985). The basement-membrane-like matrix of the mouse EHS tumor: II. Immunohistochemical quantitation of six of its components. *Am. J. Anat.* **174**, 387-398.

Grieder, N. C., Caussinus, E., Parker, D. S., Cadigan, K., Affolter, M. and Luschnig, S. (2008). gammaCOP is required for apical protein secretion and epithelial morphogenesis in Drosophila melanogaster. *PLoS ONE* **3**, e3241.

Hughes, H. and Stephens, D. J. (2008). Assembly, organization, and function of the COPII coat. *Histochem. Cell Biol.* **129**, 129-151.

Ivanov, A. I., Hopkins, A. M., Brown, G. T., Gerner-Smidt, K., Babbin, B. A., Parkos, C. A. and Nusrat, A. (2008). Myosin II regulates the shape of three-dimensional intestinal epithelial cysts. *J. Cell Sci.* **121**, 1803-1814.

Jaffe, A. B., Kaji, N., Durgan, J. and Hall, A. (2008). Cdc42 controls spindle orientation to position the apical surface during epithelial morphogenesis. *J. Cell Biol.* **183**, 625-633.

Jayaram, S. A., Senti, K. A., Tiklova, K., Tsarouhas, V., Hemphala, J. and Samakovlis, C. (2008). COPI vesicle transport is a common requirement for tube expansion in Drosophila. *PLoS ONE* **3**, e1964.

Kedinger, M., Lefebvre, O., Duluc, I., Freund, J. N. and Simon-Assmann, P. (1998). Cellular and molecular partners involved in gut morphogenesis and differentiation. *Philos. Trans. R. Soc. Lond. B Biol. Sci.* **353**, 847-856.

Kuehn, M. J., Herrmann, J. M. and Schekman, R. (1998). COPII-cargo interactions direct protein sorting into ER-derived transport vesicles. *Nature* **391**, 187-190.

Long, K. R., Yamamoto, Y., Baker, A. L., Watkins, S. C., Coyne, C. B., Conway, J. F. and Aridor, M. (2010). Sar1 assembly regulates membrane constriction and ER export. *J. Cell Biol.* **190**, 115-128.

Martin-Belmonte, F., Yu, W., Rodriguez-Fraticelli, A. E., Ewald, A. J., Werb, Z., Alonso, M. A. and Mostov, K. (2008). Cell-polarity dynamics controls the mechanism of lumen formation in epithelial morphogenesis. *Curr. Biol.* **18**, 507-513.

Matsuoka, K., Orci, L., Amherdt, M., Bednarek, S. Y., Hamamoto, S., Schekman, R. and Yeung, T. (1998). COPII-coated vesicle formation reconstituted with purified coat proteins and chemically defined liposomes. *Cell* **93**, 263-275.

Matsuoka, K., Schekman, R., Orci, L. and Heuser, J. E. (2001). Surface structure of the COPII-coated vesicle. *Proc. Natl. Acad. Sci. USA* **98**, 13705-13709.

Mellman, I. and Nelson, W. J. (2008). Coordinated protein sorting, targeting and distribution in polarized cells. *Nat. Rev. Mol. Cell Biol.* **9**, 833-845.

Mironov, A. A., Beznoussenko, G. V., Trucco, A., Lupetti, P., Smith, J. D., Geerts, W. J., Koster, A. J., Burger, K. N., Martone, M. E., Deerinck, T. J. et al. (2003). ER-to-Golgi carriers arise through direct en bloc protrusion and multistage maturation of specialized ER exit domains. *Dev. Cell* **5**, 583-594.

Norum, M., Tang, E., Chavoshi, T., Schwarz, H., Linke, D., Uv, A. and Moussian, B. (2010). Trafficking through COPII stabilises cell polarity and drives secretion during Drosophila epidermal differentiation. *PLoS One* **5**, e10802.

O'Brien, L. E., Jou, T. S., Pollack, A. L., Zhang, Q., Hansen, S. H., Yurchenco, P. and Mostov, K. E. (2001). Rac1 orientates epithelial apical polarity through effects on basolateral laminin assembly. *Nat. Cell Biol.* **3**, 831-838.

O'Donnell, J., Maddox, K. and Stagg, S. (2010). The structure of a COPII tubule. *J. Struct. Biol.* **173**, 358-364.

Rossi, M., Morita, H., Sormunen, R., Airenne, S., Kreivi, M., Wang, L., Fukai, N., Olsen, B. R., Tryggvason, K. and Soininen, R. (2003). Heparan sulfate chains of perlecan are indispensable in the lens capsule but not in the kidney. *EMBO J.* **22**, 236-245.

Saito, K., Chen, M., Bard, F., Chen, S., Zhou, H., Woodley, D., Polischuk, R., Schekman, R. and Malhotra, V. (2009). TANGO1 facilitates cargo loading at endoplasmic reticulum exit sites. *Cell* **136**, 891-902.

Salama, N. R., Chuang, J. S. and Schekman, R. W. (1997). Sec31 encodes an essential component of the COPII coat required for transport vesicle budding from the endoplasmic reticulum. *Mol. Biol. Cell* **8**, 205-217.

Schmidt, K. and Stephens, D. J. (2010). Cargo loading at the ER. *Mol. Membr. Biol.* **27**, 398-411.

Simon-Assmann, P., Lefebvre, O., Bellissent-Waydelich, A., Olsen, J., Orian-Rousseau, V. and De Arcangelis, A. (1998). The laminins: role in intestinal morphogenesis and differentiation. *Ann. N. Y. Acad. Sci.* **859**, 46-64.

Stagg, S. M., Gurkan, C., Fowler, D. M., LaPointe, P., Foss, T. R., Potter, C. S., Carragher, B. and Balch, W. E. (2006). Structure of the Sec13/31 COPII coat cage. *Nature* **439**, 234-238.

Stagg, S. M., LaPointe, P., Razvi, A., Gurkan, C., Potter, C. S., Carragher, B. and Balch, W. E. (2008). Structural basis for cargo regulation of COPII coat assembly. *Cell* **134**, 474-484.

Timpl, R. (1996). Macromolecular organization of basement membranes. *Curr. Opin. Cell Biol.* **8**, 618-624.

Townley, A. K. and Stephens, D. J. (2009). Vesicle coating and uncoating – controlling the formation of large COPII-coated carriers. *F1000 Biol. Rep.* **1**, 65.

Townley, A. K., Feng, Y., Schmidt, K., Carter, D. A., Porter, R., Verkade, P. and Stephens, D. J. (2008). Efficient coupling of Sec23-Sec24 to Sec13-Sec31 drives COPII-dependent collagen secretion and is essential for normal craniofacial development. *J. Cell Sci.* **121**, 3025-3034.

Tsarouhas, V., Senti, K. A., Jayaram, S. A., Tiklova, K., Hemphala, J., Adler, J. and Samakovlis, C. (2007). Sequential pulses of apical epithelial secretion and endocytosis drive airway maturation in Drosophila. *Dev. Cell* **13**, 214-225.

Weston, C. A., Anova, L., Rialas, C., Prives, J. M. and Weeks, B. S. (2000). Laminin-1 activates Cdc42 in the mechanism of laminin-1-mediated neurite outgrowth. *Exp. Cell Res.* **260**, 374-378.

Wilson, D. G., Phamluong, K., Li, L., Sun, M., Cao, T. C., Liu, P. S., Modrusan, Z., Sandoval, W. N., Rangell, L., Carano, R. A. et al. (2011). Global defects in collagen secretion in a Mia3/TANGO1 knockout mouse. *J. Cell Biol.* **193**, 935-951.